

This Page Is Inserted by IFW Operations
and is not a part of the Official Record

BEST AVAILABLE IMAGES

Defective images within this document are accurate representations of the original documents submitted by the applicant.

Defects in the images may include (but are not limited to):

- BLACK BORDERS
- TEXT CUT OFF AT TOP, BOTTOM OR SIDES
- FADED TEXT
- ILLEGIBLE TEXT
- SKEWED/SLANTED IMAGES
- COLORED PHOTOS
- BLACK OR VERY BLACK AND WHITE DARK PHOTOS
- GRAY SCALE DOCUMENTS

IMAGES ARE BEST AVAILABLE COPY.

**As rescanning documents *will not* correct images,
please do not report the images to the
Image Problem Mailbox.**

PROCEEDINGS OF SPIE



SPIE—The International Society for Optical Engineering

Optical Microlithography XIV

Christopher J. Progler

Chair/Editor

27 February–2 March 2001

Santa Clara, USA

Sponsored and Published by

SPIE—The International Society for Optical Engineering

Cooperating Organizations

SEMI—Semiconductor Equipment and Materials International
International SEMATECH

12-05-01 14:19 IN



Volume 4346
Part One of Two Parts

SPIE is an international technical society dedicated to advancing engineering and scientific applications of optical, photonic, imaging, electronic, and optoelectronic technologies.

SCAA mask exposures and Phase Phirst design for 110nm and below

Marc D. Levenson^a, Takeaki (Joe) Ebihara^b & Mikio Yamachika^c

^aM.D. Levenson Consulting, Saratoga, CA 95070,

^bCanon USA, Inc., Irving, TX 75063 USA,

^cJSR Microelectronics, Inc., Sunnyvale, CA 94089

ABSTRACT

The Sidewall Chrome Alternating Aperture (SCAA) mask has now successfully printed resist images with k_1 factors as low as 0.20, without significant focus-dependent spacewidth alternation or other anomalies that affect common alternating-PSM structures. The SCAA mask process (reported at BACUS 2000¹) etches the phase topography first and then forms the transparent openings that define the image in a conformal chrome layer deposited afterwards. This process minimizes the differences between the 3-dimensional environments of the phase shifted and unshifted mask features. With all chrome supported and all quartz walls covered, only the size of a chrome aperture determines its transmission and only the height difference of the quartz surface affects the phase shift. SCAA masks are more stable mechanically than alt-PSM structures in which the quartz walls are undercut beneath the chrome edges to minimize the trench walls effects. The chrome covering the phase edges also buries entire classes of unrepairable phase defects.

Initial experiments on Canon ES2 and ES3 exposure tools confirm that KrF SCAA masks project acceptable images of isolated line and line-space patterns down to ~100nm in 280nm thick JSR M108Y resist. The process windows, however, were limited by resist collapse, and there were strong optical proximity effects. Comparing the resist results to SEM scans of the masks confirmed the insensitivity of the image to overlay errors, so long as the phase steps were covered by chrome.

The Phase Phirst paradigm exploits the SCAA mask structure to enable low cost strong PSMs. The key is to mass produce SCAA mask substrates with generally useful phase topographies using wafer fab techniques. These Phase Phirst substrates would arrive at the mask houses ready to write and guaranteed to be free of phase-defects. At design houses, Phase Phirst-enabled EDA tools would lay out the chips in such a way that all fine dark features lie at the predetermined phase shift locations on the Phase Phirst substrate while the larger-dimension structures appear on a more conventional trim-mask. Once the GDS-II tapes arrive at the mask house, the chip design would be matched to the specified Phase Phirst substrate and printed in the chrome. Cost and turn around time should be similar to those of a COG mask pair. The wafer yield and resolution, however, would be enhanced by the well-known advantages of strong phase-shifting.

Keywords: Phase Shift Mask, Alt-PSM, Design, Low cost.

1. THE PHYSICS AND ECONOMICS OF STRONG PHASE SHIFT

Dual-exposure dark-field PSMs are beginning to be adopted in semiconductor manufacturing, but today's strong PSMs still show imaging anomalies, are hard to produce in quantity and are too expensive for low volume ASIC applications. These problems are intrinsic to the physics and economics of the strong PSM structures presently produced. The recently introduced SCAA mask structure and the Phase Phirst design paradigm overcome these problems¹. The purpose of this paper is to introduce these concepts to the lithography community, describe recent successes in SCAA mask fabrication and imaging and solicit partners in developing the low cost Phase Phirst paradigm.

The SCAA mask shown in figure 1(a) differs from the more common dual-trench and undercut PSM designs in that the chrome layer which defines the transmission pattern conformally covers the surface topography which creates the phase shift. That means that the chrome layer must be deposited after the reticle surface has been etched to produce the phase shift. However, doing that makes the immediate environments of the 0° and 180° spaces physically identical. The imaging anomalies which plague other structures, such as differences in transmission between 0° and 180° spaces and spacewidth-dependent phase shift, disappear.

^a muddle@aol.com; 19868 Bonnie Ridge Way, Saratoga, CA 95070

Figure 1(a) also shows that the electric field amplitudes at equal distances below the 0° and 180° space of the SCAA mask are identical, which is not the case for the dual trench structure in figure 1(b). In addition, the image brightness of the SCAA mask is improved since the transmission of spaces is controlled only by the chrome apertures and not by the bottoms and walls of the phase trenches. While the undercut alt-PSM design shown in figure 1(c) reduces the imaging asymmetries and improves the brightness it does so by reducing the adhesion of the chrome layer to the undercut substrate. The net result is a reticle that cannot be cleaned or repaired.

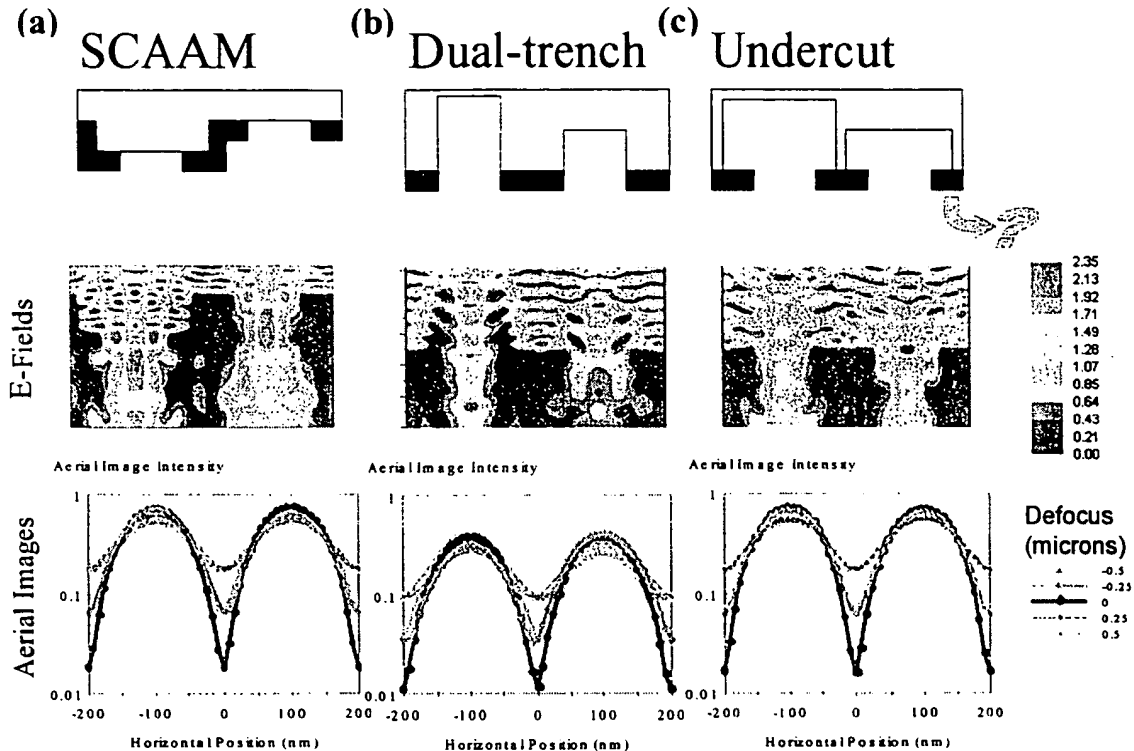


Figure 1. Rigorous electric field simulations at the reticle plane and aerial images through focus for 100nm line – 100 nm space patterns fabricated as a SCAA mask (a), dual trench PSM (b) and undercut PSM (c) as imaged at 248nm, NA=0.744, 4x and $\sigma = 0.2$ ($k_1=0.30$). The aerial image brightness is shown on a logarithmic scale to emphasize the effect of phase error. These calculations were performed using ProMAX/2D and ProLITH/2 from FINLE Technologies.

Figure 1 also shows that the intensity minima projected by the dual trench mask shift with defocus. This is the signature effect of phase error, which can occur even when the trench depth is patterned correctly. The physics of light propagation in confined structures, such as the phase trenches, causes the actual phase shift accumulated to depend on the width of the trench. Essentially, light propagating along the quartz trench walls is retarded and scattered more than light in free space. The undercut PSM design attempts to eliminate this light at the chrome layer, but that requires an undercut of more than 85nm, leaving insufficient chrome-quartz contact for structures intended to print 100nm dark lines². In contrast, the SCAA mask introduces the phase-shift through free-space propagation of light that has passed through the opaque chrome layer. Only the height of the steps in the reticle surface affects the phase shift, just as only the width of the openings in the chrome layer controls the transmission.

Figure 2 plots the phase shift and average space transmission for the three types of PSM as a function of pitch for line-space patterns with 100nm dark lines. The dual trench and undercut designs have been optimized for the 100nm line-200nm space (300nm pitch) pattern. Nevertheless, it is clear that both the transmission and phase shift of the dual-trench pattern vary in ways that complicate the design and OPC processes and limit the imaging advantages of this system. On the other hand, the SCAA mask (which does not require geometrical correction) reproduces the excellent behavior of the undercut design,

mask
SCAA
is and
es and
ilt is a

without the yield-limiting delicacy of that structure. In all cases, the predicted in-focus difference in brightness between 0° and 180° spaces is less than 5%. More detailed comparisons of simulations of different PSM structures appear in the paper by Petersen *et al.*³

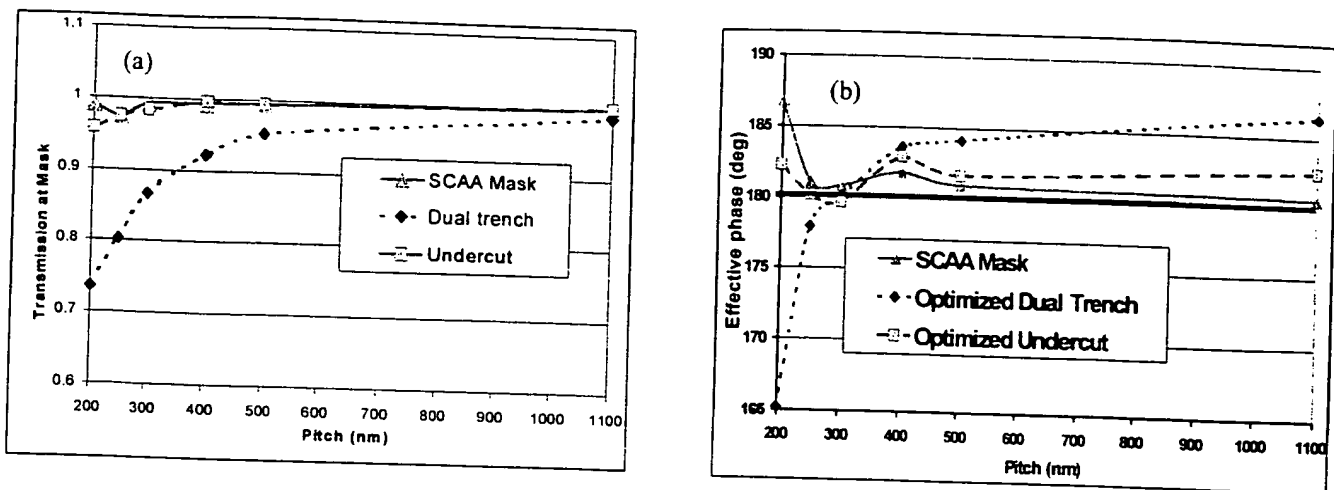


Figure 2. Pitch dependence of absolute transmission (a) and phase error (b) for SCAA, dual trench and undercut PSM designs for 100nm lines. The SCAA mask uses the geometrically-correct trench depth while the undercut and dual trench designs have the phase depth optimized for 300nm pitch (1:2 duty factor). Constant 180° phase shift prevents focus-dependent space-width alternation and image shift.¹

While the theoretical advantages of the SCAA mask structure have been known for some time,⁴ fabrication difficulties related to the behavior of available e-beam resists have only been overcome recently.¹ Briefly, the advent of 50keV mask writing tools, high-contrast resists (such as ZEP-7000) and e-beam simulation software allowed mask fabricators to anticipate and largely overcome the effects of the varying resist thickness over topography. The widths of the 0° and 180° spaces are equal on the latest reticle to 5nm and the walls are extremely vertical as shown in figure 3.

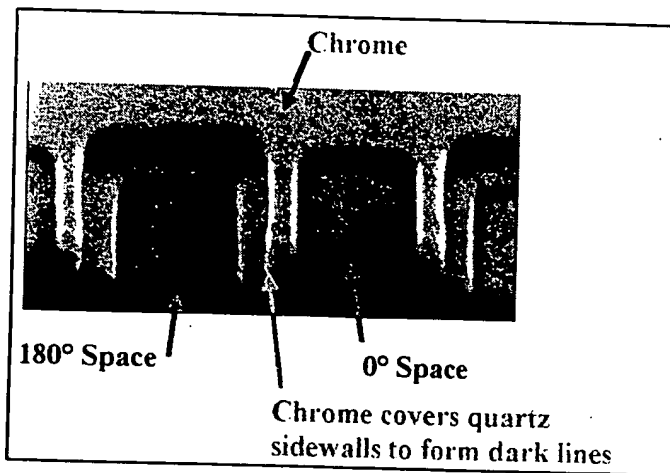


Figure 3. An SEM of an FIB-machined SCAA mask structure designed to pattern 100nm lines with 200nm spaces at 4x.

The present high cost of alternating-PSMs has three components:

1. Multiple write and etch steps with less-than-perfect yield,
2. Difficulty of inspection,
3. Impossibility of repair.

A conventionally designed SCAA mask requires as many (or perhaps more) process steps than other PSM fabrication systems. However, since the steps with the lowest yield and greatest difficulty in repair occur early, there is less value lost through imperfect yield. In particular, since the phase pattern is etched into a virgin substrate, rather than an expensively patterned mask, one can imagine economically repairing or recycling substrates with defective phase topography if the error is detected in time. Many phase etch anomalies that plague other systems are simply buried under the deposited chrome. The conformal chrome layer also will obliterate or compensate for some repair-induced anomalies, such as "riverbeds" and perhaps gallium stains. Figure 4 shows some defect and repair syndromes that will not cause problems for SCAA masks, but would be horrendous for other structures. However, some things cannot be fixed. Recycling an unrepairable SCAA mask substrate and starting over would cost less than half the expense of discarding a completed PSM. Thus, when yield is less than ~50%, the SCAA mask system may be economically advantageous.

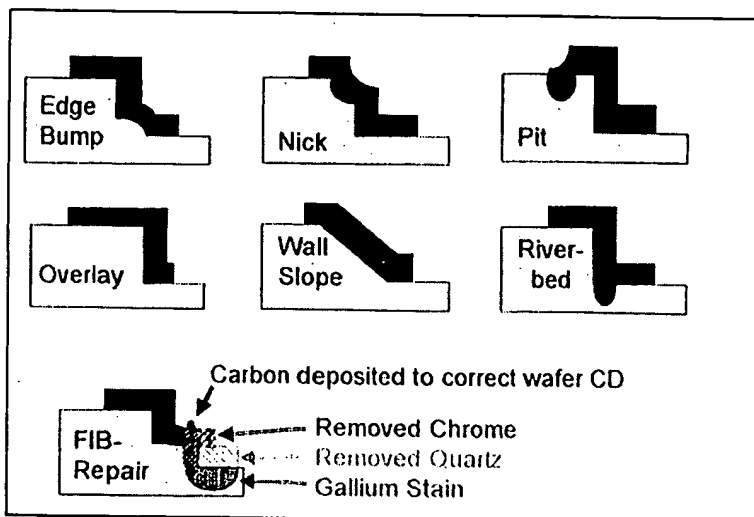


Figure 4. Buried phase defects and corrected phase repair imperfections

Since the conductive and electron-reflective chrome layer covers all phase-steps, missing shifter and other fabrication errors can be detected by top-down SEM measurement of the final mask. An AFM can also measure the topography responsible for the phase shift directly. Pinholes, mouse-bites and other chrome patterning errors can be repaired since the chrome layer is in contact with the substrate everywhere. Errors in the chrome layer cannot induce unrepairable phase defects, since the phase layer is patterned first in the SCAA mask process. It is conceivable that FIB tools may be able to repair phase errors on completed masks by machining entire windows to a 180° or 360° phase level and then etching or re-depositing opaque material to closely approximate the correct transmission. Because strong-PSMs suppress the MEEF, these repairs need not be made to the precision required for COG masks intended to project images with the same dimension. Thus it may be that SCAA masks will prove more economical than other strong PSM structures at the 100nm node and beyond.

However, PSMs that require mask-makers to perform two custom write and etch steps may always be too expensive for market segments (such as ASICs) where typical production runs are less than 500 wafers per mask. The Phase Phirst PSM paradigm is intended to lower costs for those segments by making strong-PSM production nearly identical to COG mask fabrication.

The differences between the technological and economic environments experienced by ASIC manufacturers and those of the DRAM and MPU houses which dominate lithography R&D motivated the effort to make two-exposure dark-field strong-PSM imaging cheaper. A simplified PSM system for ASICs that would facilitate lower costs, higher switching speed and greater die yield but require compromised design flexibility and circuit density might still prove acceptable. Time-to-market, not circuit density, is the key to profitability for ASIC houses.

2. THE PHASE PHIRST PARADIGM

The key to the Phase Phirst PSM Paradigm is for the mask maker to begin production with a mask substrate having a pre-patterned phase layer underneath opaque chrome and resist films and use it to make a SCAA mask compatible with the

phase-shift locations. The mask maker undertakes only a single write and a single chrome etch as for a conventional COG mask. This simplified process should result in SCAA masks with turn-around times comparable to COG masks and a cost increase related only to the value added by the pre-patterned phase blank. Standard blanks of this sort would be manufactured in 1000 plate quantities using wafer fab technologies. Since the ASIC industry is familiar with cell-based design concepts, it may also accept new chip design strategies compatible with pre-patterned PSM blanks.

A chip designed for Phase Phirst production would have all its fine features on sites chosen from a regular grid that is compatible with one of several standard substrate patterns. Larger features – which would not require phase-shift to print properly – could be placed randomly on a trim mask. The PSM in the Phase Phirst paradigm would be mostly opaque, a dark field PSM with windows opened only on opposite sides of narrow dark features. A second exposure using a COG or attenuated PSM would create the connection pattern allowing the chip to function. In the fab, this Phase Phirst Paradigm would resemble the dark-field dual exposure PSM lithography methods that are already being applied.^{5,6} Figure 5 shows how the same circuit cell can be made using various phase patterns. The inverse is also true — a single substrate phase pattern can produce many different circuit structures with different chrome openings and blockout masks. In fact, if all gates can be oriented in the same direction, a simple phase stripe pattern may prove sufficient. Of course, the circuits designed for such substrates may also be patterned successfully (but more expensively) using dipole illumination, and attenuated-PSMs!

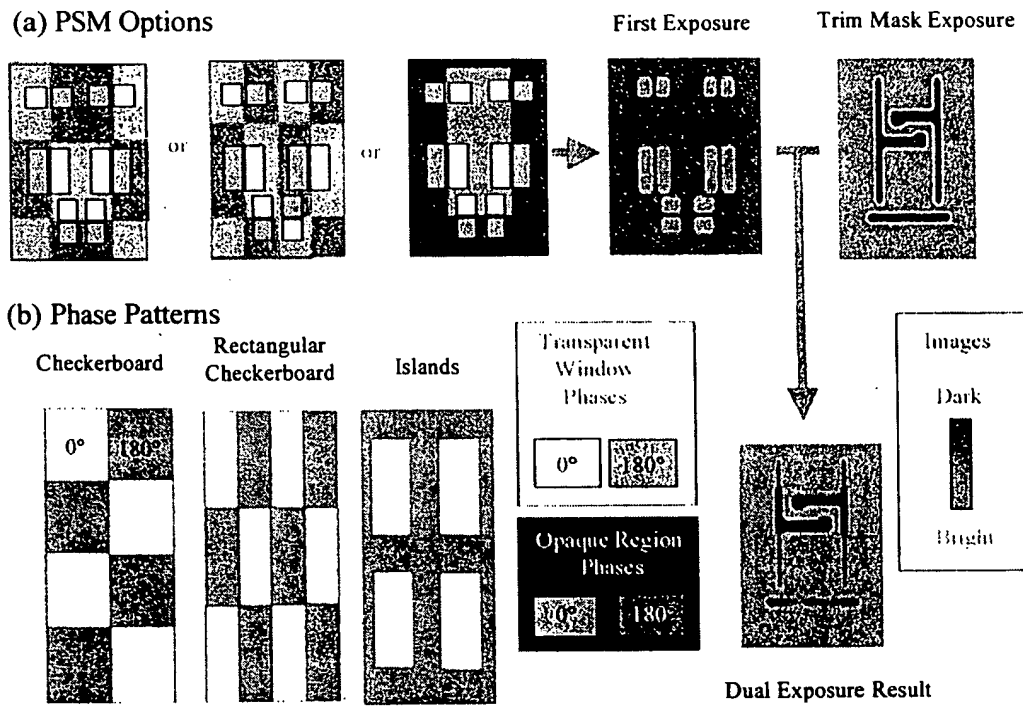


Figure 5. The same circuit cell can be printed with the same transmission windows (a) and trim-mask using any of several substrate phase patterns (b) in the Phase Phirst PSM paradigm.

The Phase Phirst substrates would be made by substrate manufacturers and supplied defect-free and coated with chrome and resist to the mask fabricators. That would not be too expensive because reject plates would be polished flat and re-used. However, if a substrate were perfect except for a few isolated anomalies, the locations of these phase-defects would be recorded in a database. Since most of the dark-field PSM will remain covered by the opaque film of chrome, it should be possible to use the defect database to match substrate and chip design so that no transparent windows are written in defective areas. The net effect would be that Phase Phirst substrates – in large volumes – would likely cost less than \$1000 more than COG substrates of similar quality.¹

The mask house would hold the Phase Phirst substrates in inventory and when a Phase-Phirst job came in, the appropriate plate would be taken from inventory and the chrome openings written using conventional technology. The mask maker would then do one write, one development, one etch, one inspection and (possibly) one repair. The overall process flow shown in

figure 6 would be nearly identical to that for a COG mask. Since the phase-shift pattern would already be in inventory, turn around should be three days or less, as for COG plates today. A trim-mask would be written at the same time to complete the dual exposure dark-field mask set. The cost to the customer should be similar to that of two COG masks! Would that be inexpensive enough for the target market? Only the market can decide, but it is unlikely that a less expensive alt-PSM paradigm will arise.

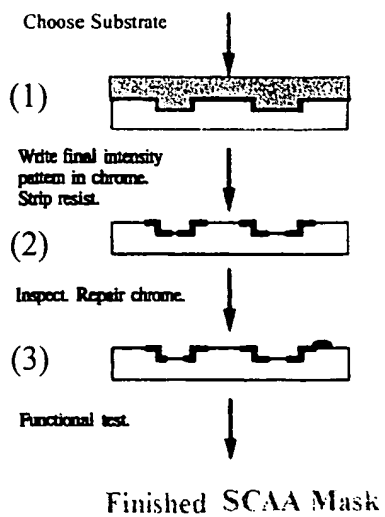


Figure 6. The steps needed to fabricate a SCAA mask using a Phase Phirst substrate.

The problem is creating sufficient demand for Phase Phirst substrates with a particular topography pattern to make their production feasible. Specialized capital equipment, such as projection aligners equipped to hold square mask substrates, will be needed to produce the Phase Phirst blanks. If only a few such blanks are made, equipment amortization will make the blank cost prohibitive. Simple estimates show that the cost of masks produced using Phase Phirst falls below that of conventional alternating PSMs at a 100 to 300 designs per topography pattern, depending on technology. Without such demand on the horizon, it is impossible to motivate the necessary investments.

Similar investments, however, will be needed to manufacture attenuated-PSMs at 193nm and 157nm and with a range of transmissions. Attenuated PSMs are key components of the other resolution enhancement strategies that promise to take optical lithography below 100nm. Given the state of the materials science supporting short-wavelength attenuated-PSM technology, the return on those investments may be even more problematical! Because of the importance of the issue, the industry needs to consider the possibility of a low cost strong-PSM option such as Phase Phirst!

3. IMAGING RESULTS

Subwavelength lithography requires an exposure tool with minimal aberrations and a highly capable resist process as well as an appropriate resolution enhancement technology. A 4x Canon FPA-5000 ES3 step and scan exposure tools performed the exposures reported here in 280nm thick JSR M108Y resist. The ES3 has an NA variable between 0.56 and 0.73 as well as partial coherence which can be set from $0.3 < \sigma < 0.85$ and total aberrations $< 0.02\lambda$ rms. In our case, the partial coherence was set to $\sigma = 0.3$ and the NA varied between NA=0.63 and NA=0.73 in 3 steps. The wafers were coated with 55nm of Brewer Science Co. DUV 42 BARC, baked for 60 seconds at 205°C prior to resist coating. The resist was prebaked at 130°C for 90 seconds and post-exposure baked at 130°C for 90 seconds before 30 second development in 0.26N TMAH. Top-down SEMs were taken using a Hitachi S9200 and cross section SEMs, with a Hitachi S4700.

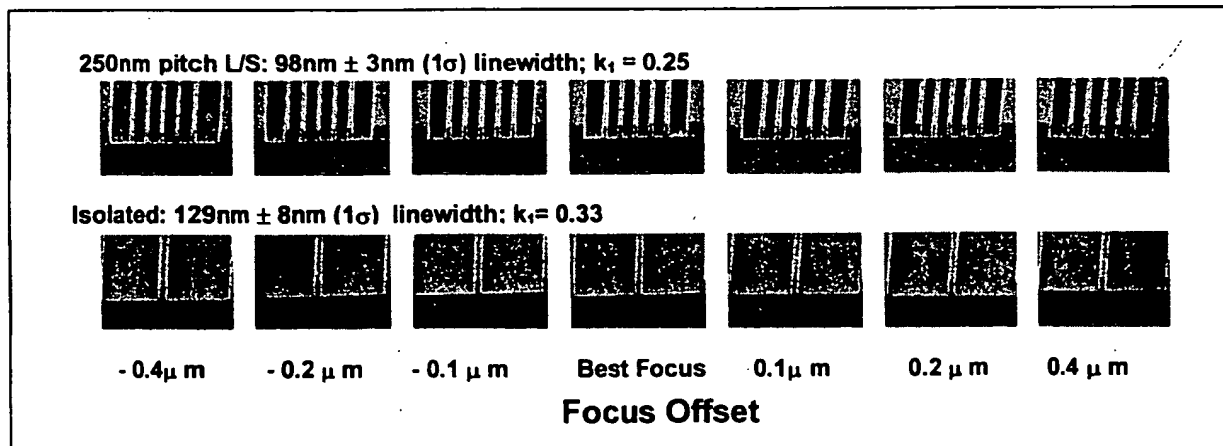


Figure 7. Cross section SEMs of 100 nm line, 150nm space 5-line patterns and nominal 100nm isolated line patterns.

Figure 7 shows typical line space (L/S) and isolated line results obtained at 320J/m^2 dose, $\text{NA}=0.63$ and $\sigma=0.3$. The 100nm line, 250nm pitch 1:1.5 duty factor line-space structure prints with $98\pm3\text{ nm}$ lines over a $0.8\mu\text{m}$ range of focus: a k_1 factor of 0.25, near the theoretical minimum. Note that the widths of the spaces are constant over the focus range. Had there been significant phase or amplitude errors, adjacent spaces would have had differing widths. The lines at the edge of the 5-line patterns also have almost the same widths as the one in the center.

Figure 7 also shows that the isolated lines printed at $129\pm8\text{nm}$ width, even though the geometrical width of the chrome would have imaged to 88nm . This large (50%) iso-dense bias is characteristic of uncorrected alternating-PSM designs.⁷ Overexposing the resist would have narrowed both the isolated and dense linewidths substantially. The process window, however, was already limited by resist collapse at 320J/m^2 and higher exposure dose would have narrowed the window, substantially. Figure 8 shows the Bossung curves for the isolated line and center line of the dense pattern. It is clear that the exposure latitude for 100nm lines in a 1:1.5 duty-factor array is larger than 6% with a $0.5\mu\text{m}$ range of focus. If the nominal CD of the isolated lines were set at 130nm (to accommodate the iso-dense bias) the process window would be even larger. The iso dense bias can perhaps be corrected using dual exposure methods or by reducing the duty factor of the dense pattern and over-exposing.

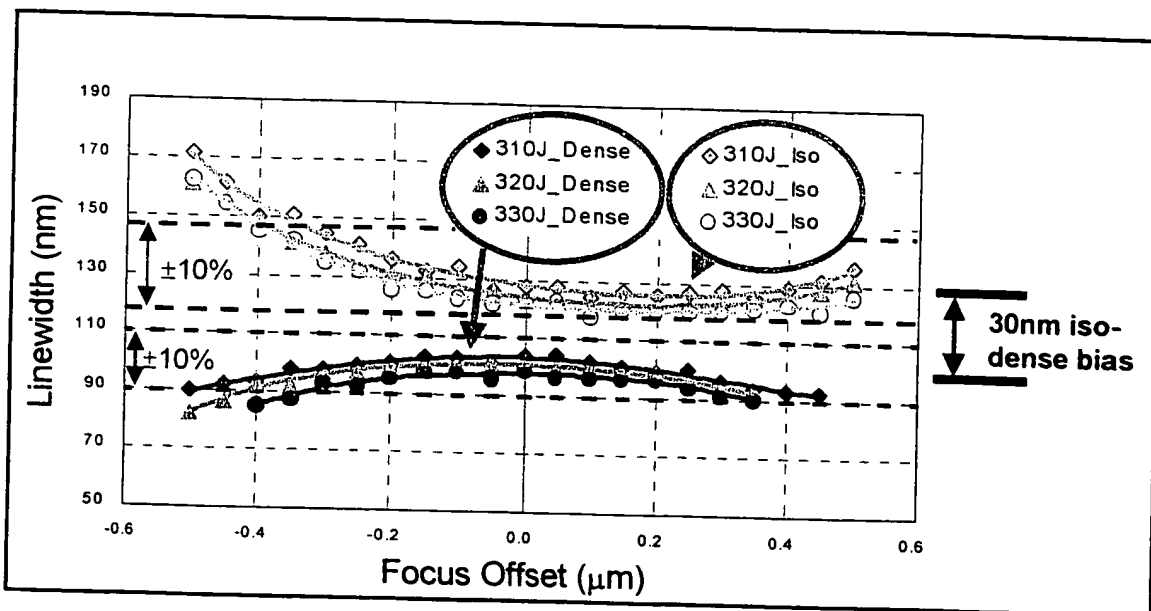


Figure 8. Bossung plots for 100nm line in the 1:1.5 duty-factor dense array and the isolated lines printed under the same conditions. The dose level is per square meter of exposed area.

Figure 9 shows Bossung plots for the 150nm 0° and 180° spaces in the 250nm pitch L/S pattern. There is no focus-dependent change in the ratio of the spacewidths as would be seen if the effective phase shift were significantly different from 180° . The fact that adjacent spaces vary in the same way with focus means that “pitch walking” – and other anomalies – that might cause image shifts are absent. On the other hand, there appears to be a just barely measurable (2-5nm) difference between the 0° and 180° spacewidths. This slight deviation is well within the error budget.

The test mask contained numerous other resolution targets, many of which have not yet been analyzed.

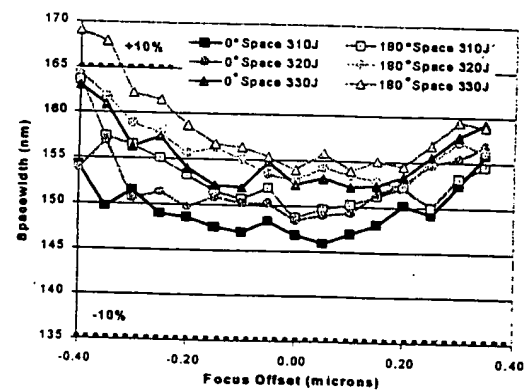


Figure 9. Bossung plots for 150nm 0° and 180° spaces in the 250nm pitch semi-dense array. The fact that these CD plots are parallel indicates the absence of anomalies such as focus-dependent spacewidth alternation at this resolution. The dose level is per square meter.

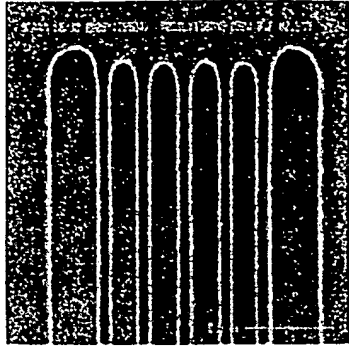


Figure 10. 82nm wide lines printed at a pitch of 220nm in 280nm thick JSR M108Y resist.

The highest resolution target was a 220nm pitch, 70nm line-150nm space array which printed as shown in figure 10 at $\text{NA}=0.68$ and $\sigma=0.30$. The process window of the 280nm thick resist was limited by resist collapse. Still, it is evident that patterns are being resolved at $k_1=0.22$ and $k_{\text{pitch}} = 0.60$.

Thinner resist reduced the collapse problem. A preliminary experiment with 210nm thick resist yielded the line and spacewidth plots shown in figure 11(a): semi-dense lines printed near the nominal 70nm width, but isolated lines were substantially larger, near 107nm, a >53% iso-dense bias! Perhaps more seriously, the widths of the 0° and 180° varied in a different fashion through focus, although the $\sim 10\text{nm}$ asymmetries were well within the $\pm 15\text{nm}$ process windows. Still, these curve suggest the presence of a $\sim 5\text{nm}$ focus-dependent image shift for the 70nm semi-dense lines. Since the overlay specifications for such features are typically 1/3 of the linewidth or $>20\text{nm}$ in this case, this minor effect should not cause serious concern.

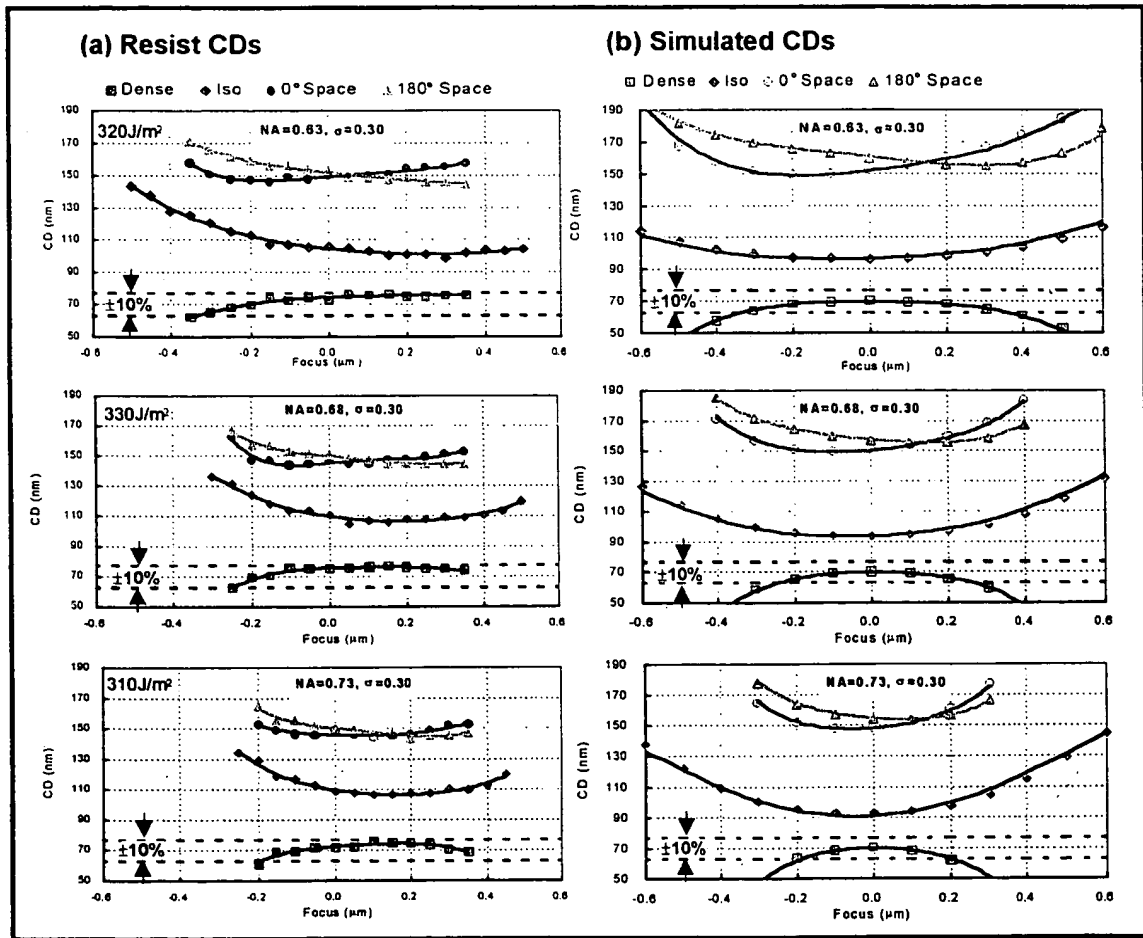


Figure 11. Line and spacewidth plots for 70nm line-150nm space patterns and 55nm (1/4 measured reticle CD) isolated lines printed in 210nm thick resist at $\text{NA}=0.63$, 0.68 and 0.73 at $\sigma=0.3$ (a), compared with electromagnetic field aerial image simulations obtained using the measured aberration parameters of the exposure tool (b)⁸.

Figure 11(b) shows the dimensions of lines and spaces in the aerial image predicted for the nominal reticle structures using the Canon in-house electromagnetic simulation program SMILE.⁸ The widths calculated represent contours of the images at the exposure level that gives the correct (70nm) linewidth for the semi-dense pattern at best focus. The solid lines in figure 11(b) correspond to the performance of a 4 \times projection tool without aberrations. The circles, squares, diamonds and triangles

represent the performance expected for a tool with the measured aberrations of the ES3. The infinitesimal deviations of the data points (that include aberrations) from the lines (which do not) indicate that the imaging predicted for the SCAA mask on the ES3 is essentially ideal at 70nm.

The qualitative and quantitative agreement between the resist CDs in figure 11(a) and the simulated aerial image CDs in 11(b) is quite remarkable, suggesting that 210nm thick resist does, in fact, follow a threshold development model and that the SCAA structure approaches (and perhaps exceeds) simple theoretical expectations of imaging performance. The resist images produced by our test SCAA mask on the Canon FPA-5000ES3 confirm that tools with very small aberrations produce nearly ideal images at 70nm, even at 220nm pitch and even with NA=0.63, a k_{pitch} value of 0.56⁹.

4. CONCLUSIONS

A Sidewall Chrome Alternating Aperture Mask has now been fabricated with vertical chrome walls and proper critical dimensions. The resist patterns obtained when this reticle was printed using a 248nm Canon ES3 step and scan exposure tool agreed with simulations based on accurate electromagnetic modeling of the diffraction and imaging processes. In particular semi-dense line-space patterns could be printed with linewidths down to 70nm and spaces as small as 150nm without significant spacewidth alternation over focus window of 0.5μm. For a 5-line 100nm line-150nm space pattern, the exposure latitude was >6% at NA=0.63 and DOF=0.5μm, limited by resist collapse. However, the widths of isolated dark lines were substantially greater and larger than the geometrical chrome widths, necessitating severe over exposure and/or optical proximity correction to achieve isolated linewidths below 130nm. Nevertheless, OPC strategies are available that should yield acceptable common process windows for dense, semi-dense and isolated lines down to 110nm and perhaps below.

While the SCAA mask structure may appear difficult to fabricate, its reparability and immunity to buried defects may make it desirable for applications requiring strong-PSM imaging at 100nm and less. Mask-shop processes can be dramatically simplified by using substrates with pre-patterned phase layers as in the Phase First PSM paradigm. If the required substrates can be made in sufficient volume, reticle costs should fall dramatically for those willing to live within the Phase First design constraints. Test patterns for Phase First have been fabricated on the two existing SCAA masks and they await proposals for the initial demonstrations.

Other methods of achieving comparable resolution are more problematical and expensive. The common single trench, undercut and dual trench alt-PSM structures must be designed carefully to cope with anomalies due to the difference between the environments of the 0° and 180° spaces. Some must be handled carefully to avoid chrome lift-off during processing and cleaning. The SCAA mask suffers from none of these difficulties. Methods which combine weak-PSMs (attenuated or tritone) with off-axis illumination may also promise 110nm imaging with reduced process windows¹⁰, but require difficult to obtain defect-free weak-PSM reticles and complex OPC.

These initial imaging results were obtained in less than an hour of tool time using un-optimized – but rather sophisticated – resist processes. Since the materials are available to make SCAA masks for 193nm illumination, one may expect to see results similar to those presented here, but with dimensions reduced by 23% as soon as adequate resists become available. In the mean time, excellent results will continue to be obtained with highly-developed 248nm tools and processes. Those who are using other methods to print resist images at the 100nm level are working too hard!

ACKNOWLEDGEMENTS

The authors wish to acknowledge the contributions that many others have made to this project. In particular, Naoya Hayashi, Yasutaka Morikawa and Haruo Kokubo of Dai Nippon Printing Co. were responsible for the SCAA mask and its characterization. We are grateful for simulations performed by Yoshiyuki Sekine of Canon Inc., Semiconductor Equipment Division, and John Petersen and David Gerold of Petersen Advanced Lithography as well as for exposure help from Yoshio Kawanobe and Kenji Saito of Canon Inc. Semiconductor Equipment Division, Utsunomiya, Japan.

REFERENCES

1. M.D. Levenson, J.S. Petersen, D.G. Gerold and Chris A. Mack, "Phase Phirst! An improved strong-PSM paradigm," *SPIE Proc.* **4186**, 395-404 (2000) and references therein.
2. T. Yamamoto, N. Ishiwata, S. Asai, "Impact of alternating phase shift mask quality on 100nm gate lithography," *SPIE Proc.* **4186-45** (2000)
3. J.S. Petersen, D.G. Gerold & M.D. Levenson, "Multiple pitch transmission and phase analysis of six types of strong phase shifting masks," *SPIE Proc.* **4346-72** (2001)
4. M.D. Levenson, "Phase-shifting mask strategies: isolated dark lines," *Microlithography World* **1**, 6-12 (March/April 1992), also Isamu Hanyu and Satoru Asai, Japanese Patents 2864601 & 3208050A2 (1991).
5. Michael E. Kling, "Phase-shifting masks come of age," *Microlithography World* **9**, 4-8 (Summer 1999).
6. Christopher Spence, Marina Plat, Emile Sahouria, Nick Cobb and Frank Schellenberg, "Integration of optical proximity correction strategies in strong phase shifter design for poly-gate layers," *SPIE Proc.* **3873**, 277-287 (1999).
7. J.S. Petersen, *et al.*, "Designing dual-trench alternating phase-shift masks for 140nm and smaller using 248nm KrF and 193nm ArF Lithography," *SPIE Proc.* **3412**, 503-520 (1998).
8. M.G. Moharam, D.A. Pommet, E. B. Grann and T.K. Gaylord, "Stable implementation of rigorous coupled wave analysis for surface-relief gratings: Enhanced transmittance matrix approach," *J. Opt. Soc. Am. A* **12**, 1077-1086 (1995) and Y. Unno, "Polarization analysis of aerial images produced by an optical lithography system," *Appl. Opt.* **37**, 1895-902 (1998).
9. John S. Petersen, "Integrated imaging: A key approach to optical lithography at 100nm+", *Solid State Technology* **44**, 80-82 (January 2001).
10. I-S. Kim, B-S. Kim, J-H. Lee, H-K. Cho & J-T. Moon, "Feasibility of very low k1 (=0.31) KrF lithography," *SPIE Proc.* **4181-05** (2000).